BNL-224512-2023-COPA

9.3 Microns: Toward a Next-Generation CO2 Laser for Particle Accelerators

M. Polyanskiy

Submitted to the Advanced Accelerator Concepts Workshop (AAC 2022) Conference
to be held at Hyatt Regency Long Island
November 06 - 11, 2022

Accelerator Test Facility

Brookhaven National Laboratory

U.S. Department of Energy

USDOE Office of Science (SC)

This work was supported by the Laboratory Directed Research and Development Program of Brookhaven National Laboratory under U.S. Department of Energy Contract No. DE-SC0012704.

DISCLAIMER

9.3 Microns: Toward a Next-Generation CO_2 Laser for Particle Accelerators

Mikhail N. Polyanskiy
Accelerator Test Facility
Brookhaven National Laboratory
Upton, NY, USA
polyanskiy@bnl.gov

Igor V. Pogorelsky
Accelerator Test Facility
Brookhaven National Laboratory
Upton, NY, USA

Marcus Babzien
Accelerator Test Facility
Brookhaven National Laboratory
Upton, NY, USA

Rotem Kupfer
Lawrence Livermore National Laboratory
Livermore, CA, USA

William Li
Accelerator Test Facility
Brookhaven National Laboratory
Upton, NY, USA

Mark A. Palmer
Accelerator Test Facility
Brookhaven National Laboratory
Upton, NY, USA

***Abstract*—We present realistic theoretical predictions of the performance of the next-generation long-wave infrared (LWIR) laser for advanced particle acceleration research at the Accelerator Test Facility (ATF) of Brookhaven National Laboratory. Two upgrades are planned for the present ATF CO_2 laser, which currently produces up to 5 TW peak power in 2 ps pulses at 9.2 µm. For the first upgrade, the deployment of a ten-millijoule solid-state seed laser at 9.3 µm will reduce the pulse duration 4 times, to 500 fs, and increase the peak power to 15 TW. The second upgrade will be the implementation of the post-compression of this pulse. This will reduce the pulse duration to three optical cycles (100 fs) and increase the usable peak power to 25 TW.**

***Index Terms*—CO_2 laser, long-wave infrared, ultrashort pulses**

I. ATF CO_2 Laser: State of the Art

ATF's long-wave infrared (LWIR) laser produces optical pulses that enable substantially different acceleration regimes compared to near-infrared lasers [1]. The best-demonstrated performance of this laser is presently a 2 ps pulse duration and a 5 TW peak power at 9.2 µm [2]. This is achieved via chirped-pulse amplification (CPA) of a microjoule seed pulse in a series of two high-pressure, mixed-isotope CO_2 laser amplifiers operating at the $9R$ branch of the CO_2 gain spectrum. A schematic of this laser's present configuration is shown in Fig. 1.

The present configuration of the laser limits the minimum pulse duration that can be achieved to 2 ps (FWHM) by a combination of two factors. The first is the shape of the gain spectrum of the high-pressure mixed-isotope CO_2 amplifiers that imprint on the spectrum of the amplified pulse. The other is an extremely high amplification, $\sim 10^{11}$, that is required to increase the pulse energy from the microjoule- to the multijoule-level ($\sim 10^7$ net amplification) and compensate for the optical losses in the system ($\sim 10^4$ mostly occurring during injection, extraction, and sixteen round-trips in the regenerative CO_2 preamplifier). Because of the high amplification, small variations in the spectral profile of the gain spectrum (Fig. 2a) dramatically affect the amplified pulse, effectively filtering out all spectral components except for a narrow region around the strongest peak (this effect is known as gain narrowing). For the active media of the amplifiers of the ATF LWIR laser, this peak corresponds to the $9R$ branch of the rotational-vibrational transitions centered at 9.2 µm. No matter how broad the spectrum of the seed pulse is, the output bandwidth is always ~ 220 GHz corresponding to a 2 ps transform-limited pulse. The spectrum and the temporal profile of the amplified pulse after the compressor are shown in Fig. 2b and Fig. 2c, respectively.

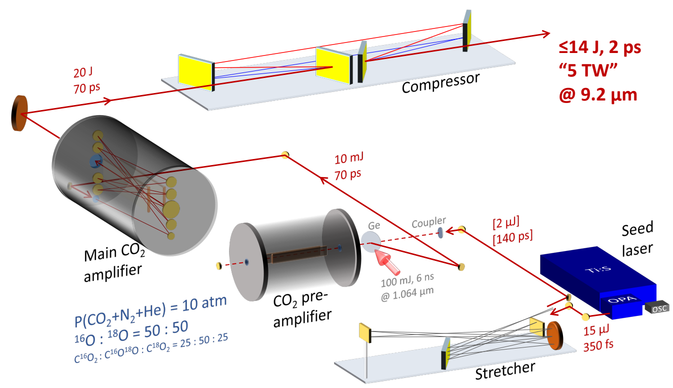

Fig. 1. Schematic of the 5 TW LWIR laser system at the ATF.

The data shown in Fig. 2 are the experimentally confirmed results of numerical simulations performed with the open-source code *co2amp* developed at the ATF [3]. We customarily apply a 20% contingency to the numerical data to account for possible imperfections in the actual system; thus, we claimed

Funding: US Department of Energy (DOE) Office of Science contract DE-SC0012704. This work was also supported by the the US DOE Accelerator Stewardship Program grant, B&R #KA2601020 (PI Mikhail Polyanskiy) and BNL Laboratory Directed Research and Development grant #20-010 AD/NPP (PI Igor Pogorelsky).

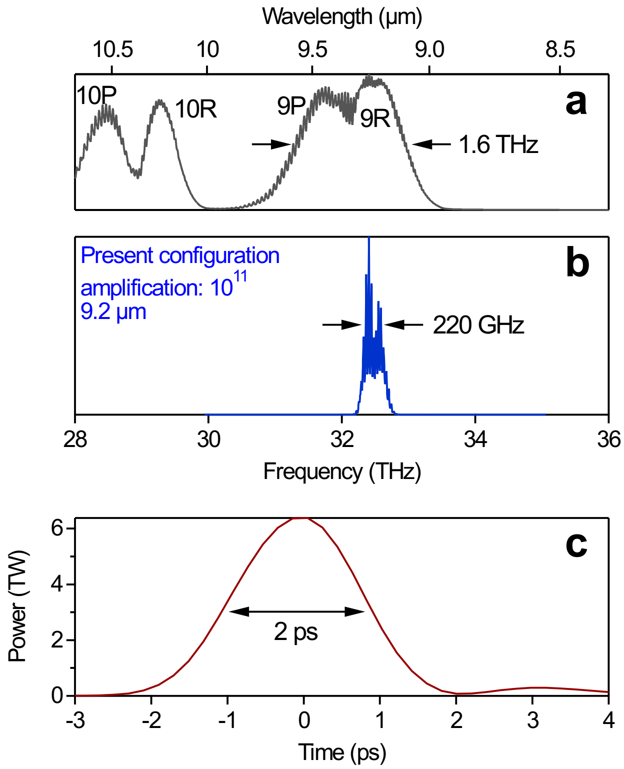

Fig. 2. Experimentally confirmed results of numerical modeling of the present configuration of the ATF CO_2 laser. The seed pulse is 1 μJ, 1 ps long, centered at 9.2 μm. a: Normalized gain spectrum. b: Normalized spectrum of the amplified pulse. c: Temporal pulse profile at the output of the system.

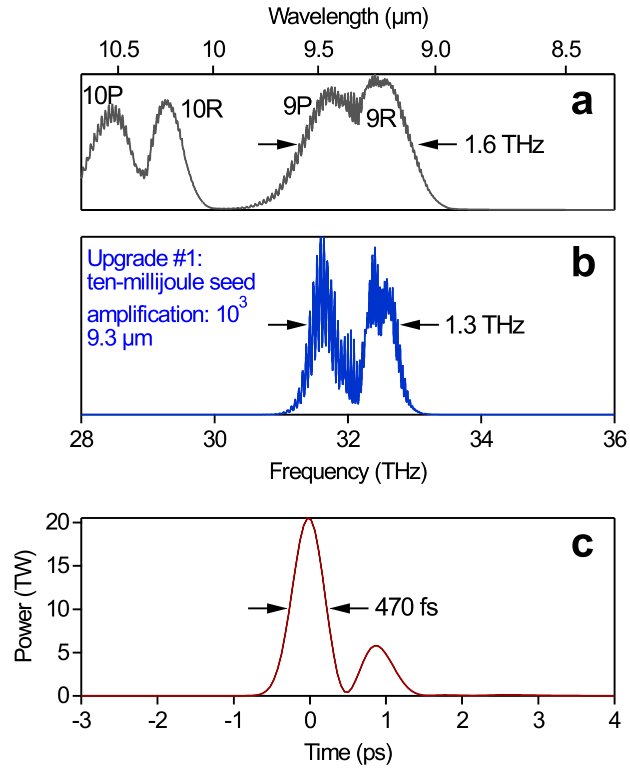

Fig. 3. Results of the numerical modeling of the CO_2 laser after the implementation of upgrade #1. The seed pulse is 10 mJ, 300 fs long, centered at 9.3 μm. a: Normalized gain spectrum. b: Normalized spectrum of the amplified pulse. c: Temporal pulse profile at the output of the system.

the achievement of 5 TW peak power despite the fact that the simulation-aided data analysis indicated a 6 TW peak [2].

II. Upgrade #1: Ten-millijoule seed

Gain narrowing can be substantially reduced if the seed pulse is strong enough to eliminate the need for pulse preamplification. For a ten-millijoule seed pulse, $\sim 10^3$ amplification in the low-loss final amplifier is sufficient to produce a multijoule output. The evolution of a spectrum of a sub-picosecond pulse overlapping two branches of the gain spectrum, $9R$ and $9P$, during this relatively small amplification is not completely out of control, as is the case for a microjoule seed. Substantial intensity is preserved in the pulse spectrum at frequencies corresponding to the weaker $9P$ branch. Moreover, once population depletion becomes considerable in a near-saturation regime, it affects the stronger $9R$ branch more than the weaker branch, thus balancing the amplification between the branches. This occurs because the red chirp of the pulse (CPA!) results in the $9R$ transitions coming into play *after* the $9P$ ones when the depletion of the shared upper laser level is more pronounced.

Fig. 3 shows the results of the numerical modeling of the amplification of a 10 mJ, 9.3 μm pulse in only the main amplifier of the ATF laser system [4]. The pulse is stretched from the original duration of 300 fs to $\sim$100 ps before the amplification and re-compressed to a transform-limited duration after the amplification.

Combining the spectral bandwidth of the $9R$ and $9P$ branches reduces the pulse duration to $\sim$500 fs while preserving the pulse energy, thus increasing peak power by nearly a factor of 4 when compared to the present configuration. Following our rule of applying a 20% contingency to numerical results, we can confidently predict a 15 TW peak power after upgrade #1 deployment.

Several schemes for generating high-energy LWIR seed pulses are currently being investigated. One was reported at this meeting by William Li of the ATF [5]. This scheme involves Raman scattering in calcite crystals followed by difference frequency generation between the Raman-shifted and non-converted leakage frequencies. Another potential approach is a multi-stage optical parametric chirped pulse amplification pumped by a mid-wave infrared laser.

III. Upgrade #2: Post-compression

The nonlinear post-compression in bulk materials demonstrated recently in the sub-TW LWIR regime [6] could potentially further reduce the pulse duration to a few optical cycles (one cycle at 9.3 μm is 31 fs). The general approach to the post-compression of a laser pulse involves two steps: 1) broadening the pulse spectrum in a nonlinear medium via self-phase modulation (SPM) and 2) compressing the intrinsically chirped SPM pulse to a near-transform-limited duration in a dispersive compressor. The LWIR post-compressor scheme developed at the ATF and shown in Fig. 4 relies on a combination of linear and nonlinear responses of two carefully chosen infrared materials, in this case KCl and BaF_2. The former has relatively strong nonlinearity and interacts with the non-compressed pulse first. The latter has lower nonlinearity but strong linear dispersion; it further broadens the spectrum while simultaneously compensating for the SPM chirp.

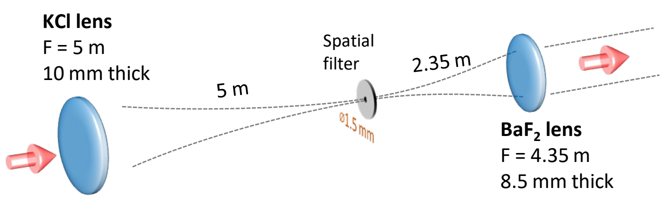

Fig. 4. Design of the post-compressor.

Nonlinear phase shift (B-integral, B) practically achievable in a single optic, is normally limited to $\sim\pi$ radians by the onset of microfilamentation. Using two bulk material components separated by a spatial filter allowed us to achieve $B \sim 2\pi$, corresponding to roughly a factor of five compression averaged across the beam. We note that the two bulk-material components in our scheme simultaneously play the role of SPM/linear-dispersion elements and serve as the focusing elements of the spatial filter.

In our numerical modeling and optimization of the post-compressor, we assumed a quasi-flattop beam with a realistic radial intensity variation and the pulse structure shown in Fig. 3 at the entrance of the first element. The output beam has a Gaussian-like profile, with considerable variation in pulse duration between the intense center and the weaker peripheral parts of the beam. The simulation results in Fig. 5b,c are the beam-averaged spectrum and temporal structure of the pulse. Because of a deviation of the beam profile from an ideal Gaussian shape and a time-dependent self-focusing in the last element of the post-compressor, the focusability of the output beam is somewhat limited. Thus, only the part of the beam that would be contained in the first diffraction maximum of the beam focus at a hypothetical interaction point is accounted for. Because of the two-stage spatial filtering (the first is the physical filtering by a hard aperture in Fig. 4, and the second is the use of only the first diffraction maximum in the final focus), a substantial part of the pulse energy is lost in this scheme. However, this is compensated for by the reduced sensitivity of the system to shot-to-shot variations in the input pulse. Spatial filters essentially select a part of the beam that is optimally compressed in the given optical configuration.

To transition from simulation results to realistic predictions, we note that in the numerical model, post-compression results in an increase in peak power at a factor of two (compare Fig. 3c and Fig. 5c). Beginning with the realistic 15 TW prediction for system performance after upgrade #1 and then multiplying it by two and applying our standard 20% contingency factor, we arrive at the $\sim$25 TW number for a realistic upgrade #2 goal.

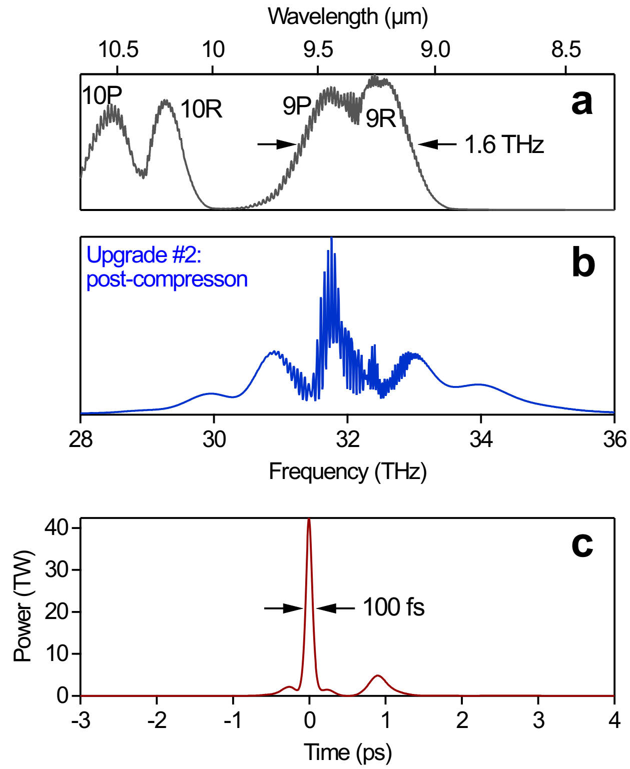

Fig. 5. Results of the numerical modeling of the post-compression LWIR laser pulse that will become available after the implementation of upgrade #1. a: Normalized gain spectrum of CO_2 amplifiers (shown for reference only). b: Normalized spectrum of the post-compressed pulse. c: Temporal profile of the usable part of the post-compressed pulse contained in the first diffraction maximum of the beam focus in the interaction point.

IV. Conclusion

Using numerical modeling backed by experimental tests and a long record of successful theoretical predictions for the performance of the laser system with mixed-isotope high-pressure CO_2 amplifiers at the ATF with the in-house developed code *co2amp*, we proposed and verified the road-map to a 25 TW, 100 fs regime of an LWIR laser at 9.3 µm. The peak power that is realistically achievable within a few years is unprecedented for optical fields at an order-of-magnitude longer wavelength compared to the majority of modern strong-field laser facilities. Combined with an expected pulse duration on the order of three optical cycles, this opens a perspective for a new class of ultra-strong-field and ultra-fast experiments. For instance, λ^2 scaling of ponderomotive potential and $\lambda^{1.7}$ scaling of x-ray cut-off energy will enable an achievement of a macroscopic-bubble laser wakefield acceleration in low-density plasma and a breakthrough to zeptosecond-bandwidth high-harmonics generation, respectively [1].

References

[1] Z. Chang et al., "Intense infrared lasers for strong-field science," Advances in Optics and Photonics, vol. 14, pp. 652–782, 2022.

[2] M. N. Polyanskiy, I. V. Pogorelsky, M. Babzien, and M. A. Palmer, "Demonstration of a 2 ps, 5 W peak power, long-wave infrared laser based on chirped-pulse amplification with mixed-isotope CO_2 amplifiers," OSA Continuum, vol. 3, pp. 459–472, 2020.

[3] M. N. Polyanskiy, "*co2amp*: A software program for modeling the dynamics of ultrashort pulses in optical systems with CO_2 amplifiers," Applied Optics, vol. 54, pp. 5136–5142, 2015. *The program with its source code is freely available at https://github.com/polyanskiy/co2amp.*

[4] M. N. Polyanskiy, I. V. Pogorelsky, M. Babzien, R. Kupfer, N. Vafaei-Najafabadi, and M. A. Palmer, "High-peak-power long-wave infrared lasers with CO_2 amplifiers," Photonics, vol. 8, p. 101, 2021.

[5] W. Li et al., "Raman-based wavelength conversion for seeding and optical pumping of CO_2 laser amplifiers," to be published in the proceedings of Advanced Accelerator Concepts 2022 workshop.

[6] M. N. Polyanskiy, I. V. Pogorelsky, M. Babzien, R. Kupfer, K. L. Vodopyanov, and M. A. Palmer, "Post-compression of long-wave infrared 2 picosecond sub-terawatt pulses in bulk materials," Optics Express, vol. 29, pp. 31714–31725, 2021.